

1 **Filtration of submicrometer particles by pelagic tunicates**

2 Kelly R. Sutherland^{a,1,2}, Laurence P. Madin^a and Roman Stocker^b

3 ^aBiology Department, Woods Hole Oceanographic Institution, 266 Woods Hole Road, Woods
4 Hole, MA 02543

5
6 ^bParsons Laboratory, Department of Civil and Environmental Engineering, Massachusetts
7 Institute of Technology, 77 Massachusetts Avenue, Cambridge, MA 02139

8
9 ¹To whom correspondence should be addressed. E-mail: krsuth@caltech.edu

10
11 ²Present address: Bioengineering, California Institute of Technology, 1200 East California
12 Boulevard, Pasadena, CA 91125

13

14 **Classification:** Biological Sciences, Ecology

15 **Manuscript Information:** 21 pages text, 5 figures, 1 table

16

17

18

19

20

21

22

23

24

25

26

27

28

1 **Abstract**

2 Salps are common in oceanic waters and have higher per individual filtration rates than any other
3 zooplankton filter feeder. Though salps are centimeters in length, feeding via particle capture
4 occurs on a fine, mucous mesh (fiber diameter $d \sim 0.1 \mu\text{m}$) at low velocity ($U = 1.6 \pm 0.6 \text{ cm s}^{-1}$,
5 mean \pm SD) and is thus a low-Reynolds number ($\text{Re} \sim 10^{-3}$) process. In contrast to the current
6 view that particle encounter is dictated by simple sieving of particles larger than the mesh
7 spacing, a low-Re mathematical model of encounter rates by the salp feeding apparatus for
8 realistic oceanic particle size distributions shows that submicron particles, due to their higher
9 abundances, are encountered at higher rates (particles per time) than larger particles. Data from
10 feeding experiments with 0.5, 1 and 3 μm diameter polystyrene spheres corroborate these results.
11 Though particles larger than 1 μm (e.g. flagellates, small diatoms) represent a larger carbon pool,
12 smaller particles in the 0.1–1 μm range (e.g. bacteria, *Prochlorococcus*) may be more quickly
13 digestible because they present more surface area, and we find that particles smaller than the
14 mesh size (1.4 μm) can fully satisfy salp energetic needs. Furthermore, by packaging
15 submicrometer particles into rapidly sinking fecal pellets, pelagic tunicates can substantially
16 change particle size spectra and increase downward fluxes in the ocean.

17 \body

18 **Introduction**

19 Filter feeding is a common strategy among marine plankton for collecting small food particles
20 from a suspension. Pelagic tunicates in the class Thaliacea, order Salpida, have the highest per
21 individual filtration rates of all marine zooplankton filter feeders (1). Weight-specific clearance
22 rates (70–4153 $\text{ml mg}^{-1} \text{ C h}^{-1}$, 2) are higher than most copepod and krill species. Salps filter feed
23 by rhythmically pumping water into the oral siphon, through the pharyngeal chamber and out the

1 atrial siphon (Fig. 1A). This pumping action, generated by circular muscle bands, also creates a
2 propulsive jet for locomotion. Food particles entering the pharyngeal chamber are strained
3 through a mucous net that is continuously secreted and rolled into a food strand that moves
4 posteriorly towards the esophagus. The bag-like net is secreted by the endostyle and fills much of
5 the pharyngeal chamber (Fig. 1A). This feeding mechanism results in ingestion of any particles
6 that enter the atrial siphon and adhere to the filtering mesh.

7 After digestion, particles are packaged into dense fecal pellets, which often contain
8 undigested or partially digested plankton (3, 4). These pellets remain intact for days (4) and have
9 sinking speeds ($200\text{--}3646\text{ m d}^{-1}$; 5, 6) that are higher than most copepod or krill pellets (3).
10 Furthermore, diurnal vertical migration by some species may accelerate vertical export (7, 8).
11 The combination of high filtration rates, small mesh size and rapid pellet sinking implies that
12 salps have the potential to shift particle distributions towards larger sizes, contribute to vertical
13 transport and remove substantial amounts of primary production from surface waters. These
14 impacts will be particularly profound following population increases, which can occur suddenly
15 under favorable conditions due to short generation times and a two-part life cycle comprising
16 asexually reproducing individuals and pseudo-colonial chains of sexually reproducing salps (1).

17 Generally, encounter rates between particles and filter elements depend on the Reynolds
18 number ($Re = dU/\nu$, where d is mesh fiber diameter, U is velocity and ν is kinematic viscosity),
19 which measures the relative importance of inertial and viscous forces. At low- Re ($Re \ll 1$)
20 viscous effects prevail and prevent flow separation around filter elements (9). Filtration in salps
21 operates in this regime, as $Re \sim 2 \times 10^{-3}$, based on mesh fiber diameter ($d \sim 0.1\ \mu\text{m}$, 10), velocity
22 at the mesh ($U = 1.6 \pm 0.6\text{ cm s}^{-1}$, mean \pm SD), and seawater viscosity ($\nu = 0.83 \times 10^{-6}\text{ m}^2\text{ s}^{-1}$).
23 Classic principles of low- Re filtration theory (9, 11) show that low- Re filter feeders can collect

1 particles smaller than the mesh spacing by relying on mechanisms other than simple sieving. The
2 primary mechanisms are direct interception of particles traveling on streamlines that come within
3 one particle radius of the filter element, and diffusional deposition caused by Brownian effects or
4 random motility, which deflect particles from streamlines and cause contact with the
5 filter. Theoretical models of caddisfly larvae (12, 13) and experiments on marine
6 appendicularians (14–16) showed encounter of particles much smaller than the mesh size via
7 diffusional deposition and direct interception, and theory suggests that other encounter
8 mechanisms (inertial impaction and gravitational deposition) are negligible for most marine filter
9 feeders (13, 17, 18). The transition from encounter to capture depends on the sticking coefficient
10 α , which represents the fraction of encountered particles that is captured.

11 Empirical studies of salp retention efficiency found a size retention cut-off of 1–2 μm , but
12 this remains inconclusive because submicrometer particles were neglected (4, 19) or
13 undetectable (20). In fact, small cyanobacteria (0.7–1 μm) have been removed by salps during
14 feeding studies (20) and identified in salp fecal pellets (3, 4). Because the smallest particles are
15 the most abundant in the ocean (Fig. 1B; 29, 30), determining the encounter efficiency of
16 submicrometer particles is of particular importance to quantify clearance rates and vertical
17 transport of particulates. Contrary to the current understanding that salps do not retain particles
18 below 1–2 μm , we show that salps can capture submicrometer particles and do so at rates that
19 exceed those of larger particles. We calculate that salps can fulfill their energetic requirements
20 with particles smaller than the mesh width and propose that they can substantially influence
21 particle size spectra in the upper ocean, increasing particle size and thus accelerating vertical
22 transport of particulate matter.

23

1 **Results**

2 Epifluorescence images revealed a regularly spaced rectangular feeding mesh (Fig. 2A) with a
3 mean mesh width and length of $W = 1.5 \pm 0.5 \mu\text{m}$ and $L = 6.0 \pm 1.5 \mu\text{m}$ ($n = 9$; mean \pm SD),
4 respectively. Some strands were oriented obliquely or possibly tangled, but their number was
5 small. Mesh width increased linearly with salp body length, L_b (Fig. 2B), as expected from an
6 isometric scaling. The use of a rectangular rather than a square mesh is common among aquatic
7 filter feeders, including appendicularians and caddisfly larvae, possibly optimizing the trade-off
8 between increasing encounter and lowering the mesh material and pressure drop (31).

9 Flow visualization provided both quantitative fluid speeds near the filter and a qualitative
10 picture of the feeding current. The mean speed (U) and maximum speed near the oral siphon
11 were 1.6 and 3.8 cm s^{-1} , respectively (Table 1). The mean speed was slightly lower than speeds
12 measured just aft of the atrial (excurrent) siphon using Particle Image Velocimetry (2.0–2.6 cm s^{-1} ;
13 32), likely because the oral siphon has a larger cross sectional area. Particle trajectories
14 showed that opening of the oral siphon resulted in the intake of fluid from around the edges of
15 the siphon (Movie S1). Upon entering the pharyngeal chamber, water accelerated and then
16 moved in a circular pattern, suggesting a tangential component of encounter between particles
17 and the filter. The observed feeding current speeds are much higher than those of
18 appendicularians (0.06–0.32 cm s^{-1} ; 17, 33), which pump fluid via sinusoidal motion of the tail,
19 and doliolids (0.11 cm s^{-1} ; 34), which rely on cilia rather than muscles to draw fluid towards a
20 mucous filter, and are of the same order as feeding currents of copepods and krill (0.6–1 cm s^{-1} ;
21 35, 36), which generate flow by the coordinated movement of feeding appendages. However,
22 salps process much higher fluid volumes than crustaceans, due to the considerably larger cross
23 sections of their feeding currents. For example, grazing pressure by a bloom of the salp *Salpa*

1 *thompsoni* in the Southern Ocean was equivalent to more than 100% of daily primary
2 production, whereas grazing by dominant copepod species was negligible (37).

3 Both diffusional deposition and direct interception play a role in determining particle
4 encounter by the filtering mesh, but direct interception is dominant for $d_p > 0.05 \mu\text{m}$ (Fig. 3). For
5 $d_p = 0.01\text{--}0.05 \mu\text{m}$ (viruses, colloids) diffusion is the primary mechanism of particle encounter,
6 though efficiency is $< 2\%$. For the smallest particles, Brownian motion results in higher
7 encounters compared to motility, whereas for $d_p > 0.2 \mu\text{m}$ diffusional deposition is larger for
8 motile microorganisms. On the other hand, swimming is unlikely for organisms smaller than 0.6
9 μm , as Brownian rotation would turn them too frequently for swimming to be effective (39). For
10 $d_p > 0.05 \mu\text{m}$, particles are more efficiently encountered via direct interception: for $0.5 \mu\text{m}$ non-
11 motile particles, encounter by direct interception is 254-fold higher than by diffusional
12 deposition, while for $1 \mu\text{m}$ motile particles that increase is 41-fold.

13 Because there are substantially higher numbers of small particles in the ocean (Fig. 1B),
14 these particles can be disproportionately ingested even when encounter efficiencies are relatively
15 low. Estimates of particle encounter (Eq. 1) based on encounter efficiency (Fig. 3) and realistic
16 particle concentrations (Fig. 1B) show that, on average, particles in the $0.01\text{--}0.1 \mu\text{m}$ size range
17 (viruses, colloids) are encountered at ~ 200 times the rate of particles in the $0.1\text{--}1 \mu\text{m}$ range
18 (submicron particles, bacteria, *Prochlorococcus*) (Fig. 4A). On the other hand, larger particles
19 still contribute more volume and carbon (Fig. 4B). The mean carbon contribution from $0.1\text{--}1 \mu\text{m}$
20 particles is 38 times larger than from $0.01\text{--}0.1 \mu\text{m}$ particles. However, $1\text{--}10 \mu\text{m}$ particles
21 contribute just four times as much carbon as $0.1\text{--}1 \mu\text{m}$ particles (Fig. 4B). If only the outer 0.1
22 μm of each particle is digested, the situation is reversed: the $0.1\text{--}1 \mu\text{m}$ size range contributes

1 20% more carbon than the 1–10 μm range, and the maximum carbon contribution comes from
2 1.1 μm particles (Fig. 4B).

3 The model shows that particles smaller than the mesh width, $W = 1.4 \mu\text{m}$, supply a total
4 of 0.15 mg C h^{-1} to a salp. The carbon ingestion rate of a 40 mm long *P. confoederata* is 2.2% of
5 the body carbon content each hour (41), or 0.02 mg C h^{-1} based on the carbon-to-body-length
6 relationship of Madin et al. (42). Therefore, even assuming that the sticking coefficient is small
7 ($\alpha = 0.1\text{--}0.2$), the carbon supplied by particles smaller than the mesh opening can support the
8 majority or entirety of the organism's carbon requirement.

9 To support this conclusion, predicted encounter rates via direct interception were tested
10 experimentally by offering particles of three sizes ($d_p = 0.5, 1$ and $3 \mu\text{m}$) to freshly collected *P.*
11 *confoederata* and quantifying the relative capture rate of particles of each size. The particle size
12 range where diffusional deposition is predicted to contribute significantly to encounter rates ($d_p <$
13 0.05 ; Fig. 3) was not tested in experiments, but its contribution in terms of carbon supply was
14 predicted to be negligible based on model results (Fig. 4). When the same concentration of each
15 particle size was offered, capture rates were similar among sizes, with a slight preference for the
16 larger particles (Fig. 5A). Relative capture rates were $29.1 \pm 8.6\%$, $30.1 \pm 5.4\%$ and $40.8 \pm$
17 12.9% (mean \pm SD) for $0.5, 1$ and $3 \mu\text{m}$ particles, respectively. They were in general agreement
18 with relative encounter rates from direct interception (relevant for particles $>0.05 \mu\text{m}$; Fig. 3),
19 predicted to be 13.8% , 32.9% and 53.3% , respectively. The discrepancy at the smallest size
20 suggests that the contribution of smaller particles is even more pronounced than the model
21 predicts. A model of simple sieving (17, 43) was an inferior predictor of relative encounter rates
22 and was particularly poor at predicting encounter rates of the smallest particles, with mean
23 relative encounter rates of 3.7% , 14.5% and 81.9% for $d_p = 0.5, 1$ and $3 \mu\text{m}$, respectively.

1 Offering a suspension of particles skewed towards higher concentrations at the smallest
2 sizes confirmed these findings: measured rates were similar to those predicted by the direct
3 interception model, and very different from the simple sieving model (Fig. 5B). In this case also,
4 experiments showed an even higher capture rate of smaller particles than anticipated from
5 modeled encounter rates. This difference could be due to a size dependence of the sticking
6 coefficient α , for example due to larger drag forces experienced by larger particles (44).

7

8 **Discussion**

9 Taken together, these results suggest that simple sieving is not the sole feeding mechanism for
10 salps and, instead, that low-Reynolds number filtering mechanisms play a major and possibly
11 dominant role by enabling salps to capture submicrometer particles. This is in stark contrast to
12 previous results, which found that salp filter feeding was characterized by a size cutoff of 1–2
13 μm (2, 10). Particles smaller than the mesh opening W were considered unimportant for feeding
14 in view of their negligible sieving efficiency, yet direct verification was hampered by
15 measurement sensitivity (2, 10). Our model results show that diffusional deposition allows
16 encounter of the smallest particles ($d_p < 0.05 \mu\text{m}$), though very inefficiently (Fig. 3). However, a
17 large fraction of submicrometer particles ($0.05 \mu\text{m} < d_p < W$) can be efficiently encountered by
18 direct interception (Fig. 4) and can largely or entirely satisfy salps' energetic requirements even
19 if the sticking coefficient α is as small as 0.1.

20 If particles were fully digested, the majority of carbon would be supplied by particles in
21 the 1–10 μm range (flagellates, small diatoms), which are primarily encountered by simple
22 sieving, still with a significant contribution of 0.1–1 μm particles (bacteria, *Prochlorococcus*)
23 encountered by direct interception. Contents of fecal pellets indicate that digestion of particles as

1 small as 1 μm is partial (3, 4) and when digestion is limited to the outer shell of the particles (e.g.
2 0.1 μm), submicrometer particles can represent the majority of the carbon supply. The thinner
3 the digested shell, the larger the contribution of smaller particles, because the nutritional value of
4 larger particles now scales with their surface area ($\sim d_p^2$), rather than volume ($\sim d_p^3$). The particle
5 size range providing the largest carbon contribution, then, results from a trade-off between
6 particle abundance decreasing and volume increasing with particle size. Yet, more experiments
7 are required to quantify the degree of digestion of various particle types and the nutritional value
8 of the digested fraction, especially considering the role of morphological and chemical properties
9 of particle coating (labile organic coatings vs. cell walls, exoskeletons, plates, spines).

10 The model calculations presented here rely on a relation for carbon content originally
11 developed for phytoplankton ($2 < d_p < 60 \mu\text{m}$; 40). It is thus important to establish whether the
12 carbon content of micron- and submicron-scale particles in the ocean is consistent with this
13 assumption. Of particular interest is the carbon content of marine colloids, which are highly
14 abundant particles in the 1 nm – 1 μm range, constituting 30–50% of 'Dissolved' Organic Carbon
15 (DOC) in the upper ocean (45). These particles originate from biological processes including cell
16 exudation (e.g. transparent exopolymers), viral infection, autolysis, egestion by flagellates, and
17 sloppy feeding (46). Thus, labile colloidal components can be rich in polysaccharides, proteins
18 and lipids (46, 47) and can play an important role in biogeochemical processes (48–50). Though
19 a conclusive understanding of the bioavailability of colloidal particles remains a major frontier
20 for biogeochemists, work conducted in several aquatic ecosystems has shown that colloids are 6–
21 37% organic carbon (median = 27%) (47). This finding is consistent with, and even somewhat on
22 the larger side of the figure for carbon content utilized here ($\sim 11\%$, based on $C_C = 0.11V^{0.99}$ [ref.
23 40] and a colloid density of $\sim 1 \text{ g ml}^{-1}$ [ref. 51]). Regardless of the nutritional value, salps

1 influence the turnover of the colloidal fraction of DOC through encounter and, ultimately,
2 assimilation or defecation.

3 Salp filtration rates are among the highest in the ocean, reaching up to 15.3 ml s^{-1} (2, 52),
4 yet, pelagic tunicates have among the smallest diameter mesh elements (see Fig. 6 in ref. 53) and
5 mesh spacing (10) of all marine filter feeders. By constantly pumping large volumes of seawater
6 through their bodies and retaining micron-scale and submicrometer particles, salps are well
7 adapted for existence in the oligotrophic ocean. Most salp species are more oceanic than neritic
8 in distribution, and high particle concentrations in coastal areas can clog their filtering apparatus
9 and disrupt feeding (54). Oceanic waters are frequently dominated by plankton that is too small
10 to be captured by sieving. The finding that salps can fulfill their energetic requirements with only
11 submicrometer particles contributes to explain this geographic distribution.

12 Carbon in the euphotic zone is typically regenerated on the order of hours via the
13 microbial loop (55). Salps and other pelagic tunicates remove particles that are four to five orders
14 of magnitude smaller than themselves, thereby bypassing several trophic levels (55). In
15 addition, muscular pumping achieves a high throughput of seawater and associated particles
16 compared to the much slower feeding currents generated by flagella or cilia in other planktonic
17 filter feeders. Particles are packaged into membrane-bound fecal pellets that are often
18 incompletely digested and therefore rich in carbon, nitrogen and phosphorous (56), and contain
19 trace elements (e.g. Ca and Mg; 4). Fecal pellets sink quickly and are transferred to a longer-
20 lived pool in deeper water, where material is sequestered on time scales of years to centuries.
21 The efficiency with which salps repackage and export carbon from surface waters suggests that
22 salps, particularly in bloom proportions, can profoundly influence biogeochemical cycling, as
23 indicated also by a recent proposition to increase global salp populations to mitigate climate

1 change (57). In summary, the high filtration rates of small particles imply that salps can rapidly
2 transfer carbon and energy from the submicron size range of the particle spectrum to higher
3 trophic levels by grazing, and to larger depths via their rapidly sinking fecal pellets. As such,
4 salps can provide a substantial shortcut to flocculation in determining the contribution of small
5 particles to vertical transport of particulate matter.

6

7 **Materials and Methods**

8 **Specimen collection.** *Pegea confoederata* were collected in individual 800 ml plastic jars using
9 blue-water SCUBA techniques (58) at the Liquid Jungle Lab off the Pacific coast of Panama (7°
10 50' N, 81° 35' W) during January 2007, 2008 and 2009. Animals were maintained in collection
11 jars or in tanks (6–11 liters) of field-collected seawater at *in situ* temperatures (26–28 °C). All
12 measurements were made within 12 h of collection.

13 **Measurements of mesh size and flow speed.** Filter mesh measurements were obtained by
14 epifluorescence microscopy. Part of the mesh of *P. confoederata* was removed by gently
15 inserting a ~1×1 mm section of a glass coverslip through the oral siphon and sweeping it through
16 the pharyngeal chamber using forceps. After adding 50–100 µl of lectin-fluorescein
17 isothiocyanate in seawater solution (1 mg ml⁻¹), the mesh was imaged using a Zeiss Axiostar
18 Plus microscope with an HBO 50 epifluorescence lamp, a 100× objective and a Nikon Coolpix
19 8800 camera. This is the first time the filtering mesh was imaged using a ‘wet’ preparation in
20 order to reduce sample distortion caused by drying and shrinking associated with TEM and SEM
21 techniques (3, 59). Data were acquired from six *P. confoederata* solitaries and three aggregates,
22 ranging from 16 to 60 mm long. Mesh length, *L*, and width, *W*, were measured in ImageJ (NIH)
23 for multiple mesh openings (mean ± SD = 16 ± 10) and averaged for each individual.

1 The flow pattern and speed were determined using particle tracking. Individual *P.*
2 *confoederata* were placed in custom-built acrylic tanks with field-collected seawater seeded with
3 $10 \pm 2 \mu\text{m}$ titanium dioxide particles. Particles were illuminated with a 1-mm-thick laser sheet
4 (30 mW, 500 nm wavelength) generated using a Powell lens (Lasiris) and their motion
5 videotaped with a Sony HDR-HC7 videocamera (1440x1080 pixels, 30 fps). Because salps are
6 transparent, particles could be tracked within the pharyngeal chamber until contact with the
7 filtering mesh occurred. Velocities were determined by tracking individual particles between
8 frames relative to landmarks on the salp body or by measuring particle streak lengths in a single
9 frame using ImageJ.

10 **Particle encounter model.** The encounter rate (60)

$$11 \quad P = \beta C = EQC \quad (\text{particles s}^{-1}) \quad [1]$$

12 is the product of the encounter rate kernel, β (ml s^{-1}), and the particle concentration, C (particles
13 ml^{-1}). Here, $\beta = EQ$, where E (dimensionless) is the capture efficiency (Supplementary
14 Information) and Q (ml s^{-1}) is the volume flow rate through the salp. Both E and C depend on
15 particle diameter, d_p . Particle capture by salps is a low-Re number process, indicating that
16 viscous forces dominate over inertial forces in determining capture. The flow through the mesh
17 has $\text{Re} = WU/\nu \sim 3 \times 10^{-2}$ and the flow around an individual mesh strand (diameter $d \sim 0.1 \mu\text{m}$;
18 10) has $\text{Re} = dU/\nu \sim 2 \times 10^{-3}$. Particle inertia is negligible, as the Stokes number $d_p^2 U \rho_p / 18 \rho \nu d$ is
19 always less than 1 for $d_p < 10 \mu\text{m}$, particle density $\rho_p = 1037 \text{ kg m}^{-3}$ and seawater density $\rho =$
20 1030 kg m^{-3} . Thus, particle capture is limited to non-inertial mechanisms, which include direct
21 interception and diffusional deposition (12).

22 We used a model for capture efficiency, E , by a rectangular mesh (Supplementary
23 Information; 12), with parameters that were directly measured (mesh dimensions, flow through

1 the filter) or taken from literature (mesh fiber diameter, particle size distribution). We assumed
2 spherical particles in Eq. 1. The encounter of non-motile and motile particles by diffusional
3 deposition was modeled by a diffusivity based on Brownian motion and random motility,
4 respectively (Supplementary Information).

5 The volume flow rate through the salp, $Q = 1.69 \text{ ml s}^{-1}$, was determined as the average
6 from three studies (20, 52, 61) and had a standard deviation of 1.44 ml s^{-1} . The particle size
7 distribution, concentration C of particles of size d_p , was obtained from four Atlantic Ocean
8 transects (28) and is likely a conservative estimate, as other studies found higher concentrations
9 in all size ranges (Fig. 1B). Carbon encounter was calculated using the relation $C_C = 0.11V^{0.99}$
10 (40) between carbon content, C_C (pg C cell⁻¹), and particle volume, V (μm³), for phytoplankton
11 (similar relations apply for bacterioplankton and colloids; 47, 62). Because partially undigested
12 particles are frequently observed in salp fecal pellets (3, 4), we also explored the implications for
13 carbon encounter if only the outer 0.1 μm of each particle is digested. Relative estimates of
14 particle and carbon encounters mentioned in the text were computed based on uniformly
15 distributed values of particle diameter with spacing of 0.01 μm.

16 **Particle capture experiments.** Relative retention efficiencies of $d_p = 0.5, 1$ and 3 μm
17 fluorescent polystyrene microspheres (Polysciences, Inc.) were determined using two feeding
18 experiments, performed within 3 h of specimen collection. Microspheres were pretreated with 5
19 mg ml^{-1} bovine serum albumin for 12–48 h to avoid clumping (63). In the first experiment,
20 microspheres were added to each jar at a concentration $C \approx 10^3 \text{ ml}^{-1}$ for each size. After 2 h, *P.*
21 *confoederata* guts were excised and ground using a mortar and pestle along with several
22 microliters of seawater. Two 2 μl subsamples of the homogenate were examined using
23 epifluorescence microscopy at $200\times$ magnification and $365 \pm 12 \text{ nm}$ excitation, and particles of

1 each size were counted from three fields of view from each 2 μl subsample. The three particle
2 sizes were distinguished based on size ($d_p = 0.5, 1$ and $3 \mu\text{m}$) and emission wavelength (486,
3 407, 486 nm, respectively). Each count included a minimum of 50 particles. In the second
4 experiment the starting concentrations were $C \approx 10^5, 10^4$ and 10^3 ml^{-1} for $d_p = 0.5, 1$ and $3 \mu\text{m}$,
5 respectively, to better represent the prevalence of small particles in the ocean (Fig. 1B). For both
6 experiments, relative retention efficiencies were determined by dividing the count for a given
7 particle size by the total count for all three sizes. Comparisons were made between relative
8 retention efficiencies from experiments, the low-Re encounter model and a simple sieving model
9 based on an experimentally determined Gaussian distribution of mesh widths (17, 43).

10

11 **ACKNOWLEDGEMENTS.** We thank those that facilitated our work at the Liquid Jungle Lab,
12 Panama, especially Ellen Bailey, Luis Camilli and numerous SCUBA divers. Mark Wells, Hugh
13 Ducklow and Dariusz Stramski, as well as two anonymous reviewers, provided insightful
14 comments relating to the manuscript. This work was supported by the National Science
15 Foundation (OCE-0647723 to LPM and OCE-074464- CAREER to RS) and the WHOI Ocean
16 Life Institute.

17

18

19 **References**

- 20 1. Alldredge AL, and Madin LP (1982) Pelagic tunicates: Unique herbivores in the marine
21 plankton. *BioScience* 32: 655-663.
- 22
- 23 2. Madin LP, Deibel D (1998) in *The biology of pelagic tunicates*, ed Bone Q (Oxford University
24 Press, New York), pp 81-103.
- 25
- 26 3. Silver MW, Bruland KW (1981) Differential feeding and fecal pellet composition of salps and
27 pteropods, and the possible origin of deep water flora and olive-green "cells". *Mar Biol* 62:
28 263-273.

- 1
- 2 4. Caron DA, Madin LP, Cole JJ (1989) Composition and degradation of salp fecal pellets:
3 Implications for vertical flux in oceanic environments. *J Mar Res* 47: 829-850.
4
- 5 5. Yoon WD, Marty JC, Sylvain D, Nival P (1996) Degradation of fecal pellets in *Pegea*
6 *confoederata* (Salpidae, Thaliacea) and its implication in the vertical flux of organic matter. *J*
7 *Exp Mar Biol Ecol* 203: 147-177.
8
- 9 6. Phillips B, Kremer P, Madin LP (2009) Defecation by *Salpa thompsoni* and its contribution to
10 vertical flux in the Southern Ocean. *Mar Biol* 156: 455-467.
11
- 12 7. Madin LP et al (2006) Periodic swarms of the salp *Salpa aspera* in the Slope Water off the NE
13 United States: Biovolume, vertical migration, grazing and vertical flux. *Deep-Sea Res I* 53:
14 804-819.
15
- 16 8. Wiebe PH, Madin LP, Haury LR, Harbison GR, Philbin LM (1979) Diel vertical migration by
17 *Salpa aspera* and its potential for large-scale particulate organic matter transport to the deep-
18 sea. *Mar Biol* 53: 249-255.
19
- 20 9. Rubenstein DI, Koehl MAR (1977) The mechanisms of filter feeding: Some theoretical
21 considerations. *Am Nat* 111: 981-994.
22
- 23 10. Bone Q, Carre C, Chang P (2003) Tunicate feeding filters. *J Mar Biol Assoc UK* 83: 907-
24 919.
25
- 26 11. Shimeta J, Jumars PA (1991) Physical mechanisms and rates of particle capture by
27 suspension feeders. *Oceanogr Mar Biol* 29: 191-257.
28
- 29 12. Silvester NR (1983) Some hydrodynamic aspects of filter feeding with rectangular mesh
30 nets. *J theor Biol* 103: 265-286.
31
- 32 13. Loudon C, Alstad DN (1990) Theoretical mechanics of particle capture: Predictions for
33 hydropsychid caddisfly distributional ecology. *Am Nat* 135: 360-381.
34
- 35 14. Deibel D, Lee SH (1992) Retention efficiency of submicrometer particles by the pharyngeal
36 filter of the pelagic tunicate *Oikopleura vanhoeffeni*. *Mar Ecol Prog Ser* 81: 25-30.
37
- 38 15. Flood PR, Deibel D, Morris CC (1992) Filtration of colloidal melanin from seawater by
39 planktonic tunicates. *Nature* 355: 630-632.
40
- 41 16. Fernández D, Lopez-Urrutia A, Fernández A, Acuña JL, Harris R (2004) Retention
42 efficiency of 0.2 to 6 μm particles by the appendicularians *Oikopleura dioica* and *Fritillaria*
43 *borealis*. *Mar Ecol Prog Ser* 266: 89-101.
44
- 45 17. Acuña JL, Deibel D, Morris CC (1996) Particle capture mechanism of the pelagic tunicate
46 *Oikopleura vanhoeffeni*. *Limnol Oceanogr* 41: 1800-1814.

- 1
- 2 18. Shimeta J (1993) Diffusional encounter of submicrometer particles and small cells by
- 3 suspension feeders. *Limnol Oceanogr* 38: 456-465.
- 4
- 5 19. Kremer P, Madin LP (1992) Particle retention efficiency of salps. *J Plank Res* 14: 1009-
- 6 1015.
- 7
- 8 20. Harbison GR, Gilmer RW (1976) The feeding rates of the pelagic tunicate *Pegea*
- 9 *confederata* and two other salps. *Limnol Oceanogr* 21: 517-528.
- 10
- 11 21. Fuhrman J (2000) in *Microbial ecology of the oceans*, ed Kirchman DL (Wiley-Liss Inc.,
- 12 New York), pp 327-350.
- 13
- 14 22. Wells ML, Goldberg ED (1994). The distribution of colloids in the North Atlantic and
- 15 Southern Oceans. *Limnol Oceanogr* 39: 286-302.
- 16
- 17 23. Yamasaki A et al. (1998) Submicrometer particles in northwest Pacific coastal environments:
- 18 Abundance, size distribution, and biological origins. *Limnol Oceanogr* 43: 536-542.
- 19
- 20 24. Caron DA et al. (1995) The contribution of microorganisms to particulate carbon and
- 21 nitrogen in surface waters of the Sargasso Sea near Bermuda. *Deep-Sea Res I* 42: 943-972.
- 22
- 23 25. Li WKW (1998) Annual average abundance of heterotrophic bacteria and *Synechococcus* in
- 24 surface ocean waters. *Limnol Oceanogr* 43: 1746-1753.
- 25
- 26 26. Partensky F, Hess WR, Vaultot D (1999) *Prochlorococcus*, a marine photosynthetic
- 27 prokaryote of global significance. *Microbiol Molec Biol Rev* 63(1): 106-127.
- 28
- 29 27. Dennett MR et al. (1999) Abundance and biomass of nano- and microplankton assemblages
- 30 during the 1995 Northeast Monsoon and Spring Intermonsoon in the Arabian Sea. *Deep-Sea*
- 31 *Res I* 46: 1691-1717.
- 32
- 33 28. Cermeño P, Figueiras FG (2008) Species richness and cell-size distribution: Size structure of
- 34 phytoplankton communities. *Mar Ecol Prog Ser* 357: 79-85.
- 35
- 36 29. Sheldon RW, Prakash A, Sutcliffe WH (1972) The size distribution of particles in the ocean.
- 37 *Limnol Oceanogr* 17: 327-340.
- 38
- 39 30. Wells ML, Goldberg ED (1991) Occurrence of small colloids in sea water. *Nature* 353: 342-
- 40 344.
- 41
- 42 31. Wallace JB, Malas D (1976) The significance of the elongate, rectangular mesh found in
- 43 capture nets of fine particle filter feeding trichoptera larvae. *Arch Hydrobiol* 77: 205-212.
- 44
- 45 32. Sutherland KR, Madin LP (In press) Jet wake structure and swimming performance of salps.
- 46 *J Exp Biol*.

- 1
2 33. Morris CC, Deibel D (1993) Flow rate and particle concentration within the house of the
3 pelagic tunicate *Oikopleura vanhoeffeni*. *Mar Biol* 115: 445-452.
4
5 34. Bone Q, Braconnot JC, Carre C, Ryan KP (1997) On the filter-feeding of *Doliolum*
6 (Tunicata: Thaliacea). *J Exp Mar Biol Ecol* 214: 179-193.
7
8 35. van Duren LA, Stambhuis EJ, Videler JJ (2003) Copepod feeding currents: flow patterns,
9 filtration rates and energetics. *J Exp Biol* 206: 255-267.
10
11 36. Yen J, Brown J, Webster DR (2003) Analysis of the flow field of the krill, *Euphausia*
12 *pacifica*. *Mar Fresh Behav Physiol* 36: 307-319.
13
14 37. Dubischar CD, Bathmann UV (1997) Grazing impact of copepods and salps on
15 phytoplankton in the Atlantic sector of the Southern Ocean. *Deep-Sea Res II* 44: 415-433.
16
17 38. Visser AW, Kiorboe T (2006) Plankton motility patterns and encounter rates. *Oecologia* 148:
18 538-546.
19
20 39. Dusenbery DB (2009) *Living at the micro scale: the unexpected physics of being small*.
21 (Harvard University Press, Cambridge).
22
23 40. Montagnes DJS, Berges JA, Harrison PJ, Taylor FJR (1994) Estimating carbon, nitrogen,
24 protein, and chlorophyll *a* from volume in marine phytoplankton. *Limnol Oceanogr* 39:
25 1044-1060.
26
27 41. Cetta CM, Madin LP, Kremer, P (1986) Respiration and excretion by oceanic salps. *Mar Biol*
28 91: 529- 537.
29
30 42. Madin LP, Cetta CM, McAlister VL (1981) Elemental and biochemical composition of salps
31 (Tunicata:Thaliacea). *Mar Biol* 63: 217-226.
32
33 43. Harbison GR, McAlister VL (1979) The filter-feeding rates and particle retention efficiencies
34 of three species of *Cyclosalpa* (Tunicata, Thaliacea). *Limnol Oceanogr* 24: 875-892.
35
36 44. Shimeta J, Koehl MAR (1997) Mechanisms of particle selection by tentaculate suspension
37 feeders during encounter, retention, and handling. *J Exp Mar Biol Ecol* 209: 47-73.
38
39 45. Guo LD, Coleman CH, Santschi PH (1994) The distribution of colloidal and dissolved
40 organic-carbon in the Gulf of Mexico. *Mar Chem* 45:105-119.
41
42 46. Nagata T, Kirchman DL (1997) in *Advances in Microbial Ecology*, ed Jones (Plenum Press,
43 New York), pp 81-103.
44
45 47. Guo L, Santschi PH (1997) Composition and cycling of colloids in marine environments. *Rev*
46 *Geophys* 35: 17-40.

- 1
2 48. Amon RMW, Benner R (1994) Rapid cycling of high-molecular-weight dissolved organic
3 matter in the ocean. *Nature* 369: 549-552.
4
5 49. Verdugo P et al. (2008) Marine biopolymer self-assembly: implications for carbon cycling
6 in the ocean. *Faraday Discuss* 139: 393-398.
7
8 50. Wells ML (2002) in *Biogeochemistry of Marine Dissolved Organic Matter*, eds Hansell DA,
9 Carlson CA (Elsevier Science, USA), pp. 367-404.
10
11 51. Dean RB (1948) *Modern colloids: An introduction to the physical chemistry of large*
12 *molecules and small particles*. (D. Van Nostrand, New York).
13
14 52. Sutherland KR, Madin LP (2010) A comparison of filtration rates among pelagic tunicates
15 using kinematic measurements. *Mar Biol* 157: 755-764.
16
17 53. Humphries S (2009) Filter feeders and plankton increase particle encounter rates through
18 flow regime control. *Proc Nat Acad Sci USA* 106: 7882-7887.
19
20 54. Harbison GR, McAlister VL, Gilmer RW (1986) The response of the salp, *Pegea*
21 *confoederata*, to high levels of particulate material: starvation in the midst of plenty. *Limnol*
22 *Oceanogr* 31: 371-382.
23
24 55. Fortier L, Lefevre J, Legendre L (1994) Export of biogenic carbon to fish and to the deep-
25 ocean: the role of large planktonic microphages. *J Plank Res* 16: 809-839.
26
27 56. Andersen V (1998) in *The biology of pelagic tunicates*, ed Bone Q (Oxford University Press,
28 New York), pp 125-137.
29
30 57. Kithil PW (2006) Are salps a silver bullet against global warming and ocean acidification?
31 *AGU Fall Meeting*, San Francisco.
32
33 58. Haddock SHD, Heine JN (2005) *Scientific blue-water diving* (California Sea Grant College
34 Program Report No. T-057).
35
36 59. Bone Q, Braconnot JC, Ryan KP (1991) On the pharyngeal feeding filter of the salp *Pegea*
37 *confoederata* (Tunicata, Thaliacea). *Acta Zool* 72: 55-60.
38
39 60. Kiørboe T (2008) *A mechanistic approach to plankton ecology* (Princeton University Press,
40 Princeton).
41
42 61. Madin LP, Kremer P (1995) Determination of the filter-feeding rates of salps (Tunicata,
43 Thaliacea). *ICES J Mar Sci* 52: 583-595.
44

- 1 62. Posch T et al (2001) Precision of bacterioplankton biomass determination: a comparison of
2 two fluorescent dyes, and of allometric and linear volume-to-carbon conversion factors.
3 *Aquat Microb Ecol* 25: 55-63.
4
5 63. Pace ML, Bailiff MD (1987) Evaluation of a fluorescent microsphere technique for
6 measuring grazing rates of phagotrophic microorganisms. *Mar Ecol Prog Ser* 40: 185-193.
7
8 64. Loudon C (1990) Empirical test of filtering theory: particle capture by rectangular-mesh nets.
9 *Limnol Oceanogr* 35: 143-148
10
11

12 **Figure Legends**

13 Fig. 1. Pelagic tunicates and particulate food. (A) Schematic of three *Pegea confoederata*
14 individuals (aggregate stage). Mucous feeding filter (normally transparent) is shaded in red and
15 direction of feeding current shown with arrows. (B) Size distribution of living and non-living
16 particles in the upper ocean, including viruses (21), colloids (22), submicron particles (23),
17 bacteria (24, 25), *Prochlorococcus* (26), *Synechococcus* (25), nanoplankton (24, 27), and
18 microplankton (24, 27). Line is regression of microphytoplankton concentration versus cell
19 diameter, $\log_{10}C = -0.91 \log_{10}(d_p^3 \pi/6) + 3.5$; C in particles ml^{-1} and d_p in μm (28). Graphic by E.
20 P. Oberlander, WHOI.
21

22 Fig. 2. Filtering mesh of *P. confoederata*. (A) Epifluorescent image of mesh. Scale bar is 5 μm .
23 (B) Mesh width, W (μm), as a function of body length, L_b (mm) ($n = 9$). The line corresponds to
24 $W = 0.02L_b + 0.58$ ($n = 9$; $r^2 = 0.70$).
25

26 Fig. 3. Particle encounter efficiency predicted for *P. confoederata* over a range of particle sizes.
27 Efficiency of direct interception (blue) is shown for the mean measured mesh width $W = 1.4 \mu\text{m}$
28 (solid line), with lower and upper bounds (dashed lines) corresponding to minimum and

1 maximum mesh widths ($W = 0.5$ and $2.3 \mu\text{m}$, respectively; Fig. 2B). Efficiency of diffusional
2 deposition is shown in green for passive particles and in red for motile microorganisms, with
3 diffusivities from Visser and Kiørboe ($D = 2.8d_p^{1.71}$, D in $\text{cm}^2 \text{s}^{-1}$ and d_p in cm , ref. 38) for the
4 latter. The red line is dashed for $d_p < 0.6 \mu\text{m}$ because motility is unlikely for organisms of that
5 size (39). Vertical grey dotted lines correspond to experimental particle sizes.

6

7 Fig. 4. Combined encounter rate predicted for direct interception and diffusional deposition
8 (passive and motile particles) as a function of particle diameter for *P. confoederata*. Calculation
9 based on Eq. 1, with E from Fig. 3, $Q = 1.69 \text{ ml s}^{-1}$ and $\log_{10}C = -0.91 \log_{10}(d_p^3 \pi/6) + 3.5$ (28;
10 Fig. 1). (A) Particle encounter rate and (B) carbon encounter rate based on $C_C = 0.11V^{0.99}$, where
11 C_C is carbon content (pg C cell^{-1}), and V is particle volume (μm^3) (40). For the latter, two cases
12 were considered: that the full particle is digested (solid line), or that only the outer $0.1 \mu\text{m}$ -thick
13 shell of each particle is digested (dashed line). Note that above $d_p = 1.2 \mu\text{m}$, direct interception
14 efficiency is 100%.

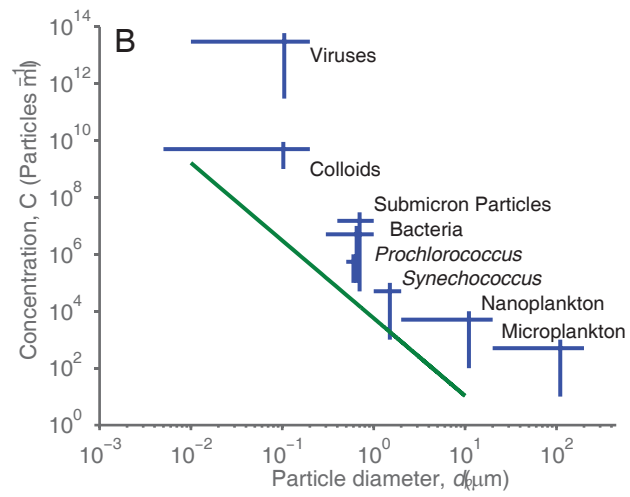
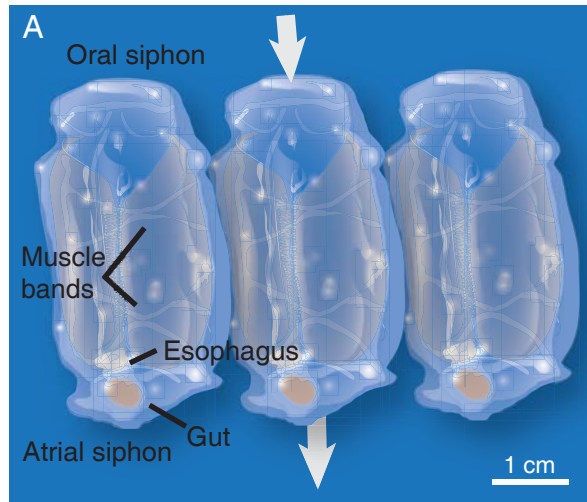
15

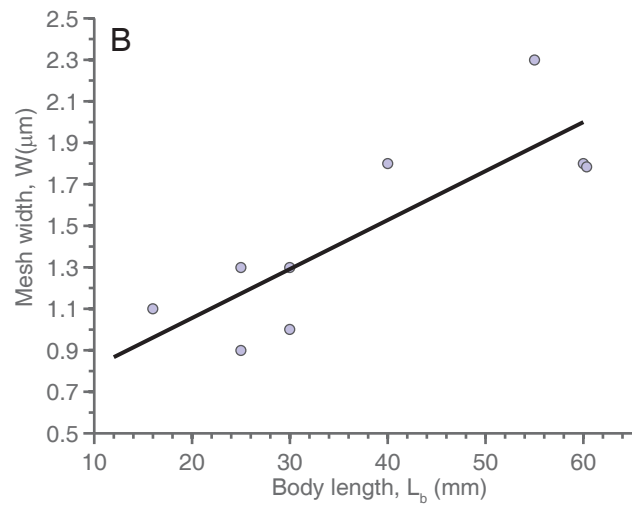
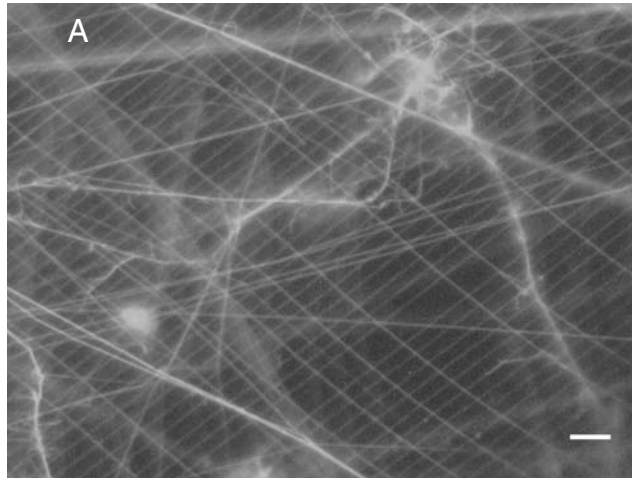
16 Fig. 5. Relative proportions of 0.5 , 1 and $3 \mu\text{m}$ microspheres in *P. confoederata* gut after feeding
17 experiments (Exp), compared to relative proportions predicted by direct interception (Dir int)
18 and simple sieving (Sieving). (A) Equal initial concentrations of each particle size class ($\sim 10^3$
19 particles ml^{-1}). (B) Higher initial concentration of smaller particles (0.5 , 1 and $3 \mu\text{m}$ particle
20 concentrations were $\sim 10^5$, $\sim 10^4$ and $\sim 10^3$ particles ml^{-1} , respectively).

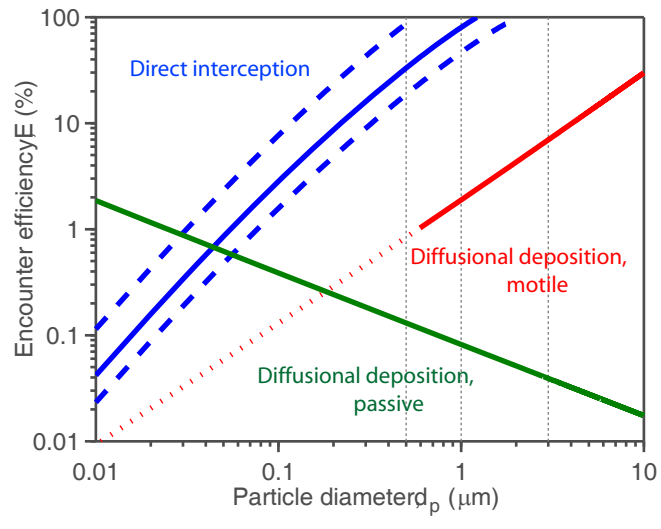
21

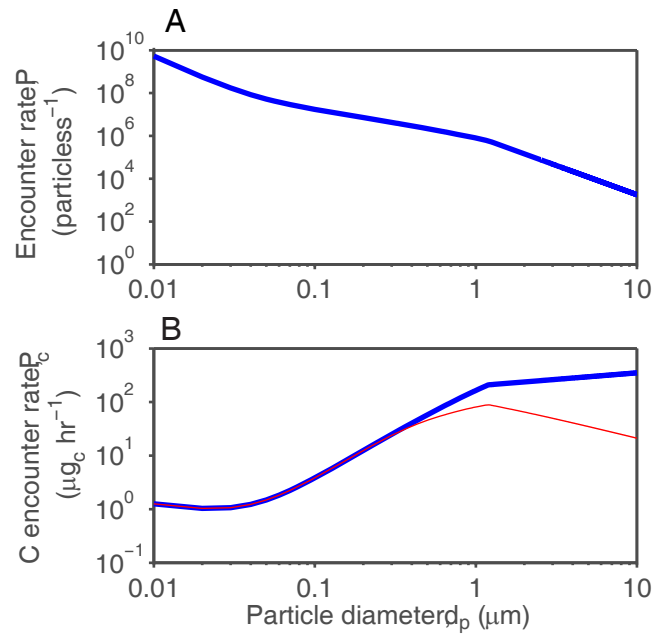
1 Table 1. Flow speed at *P. confoederata* feeding filter. Values expressed as mean \pm SD, with
2 number of measurements in parenthesis. The mean speed weighted by the number of
3 measurements for each organism was $1.5 \pm 1.1 \text{ cm s}^{-1}$.

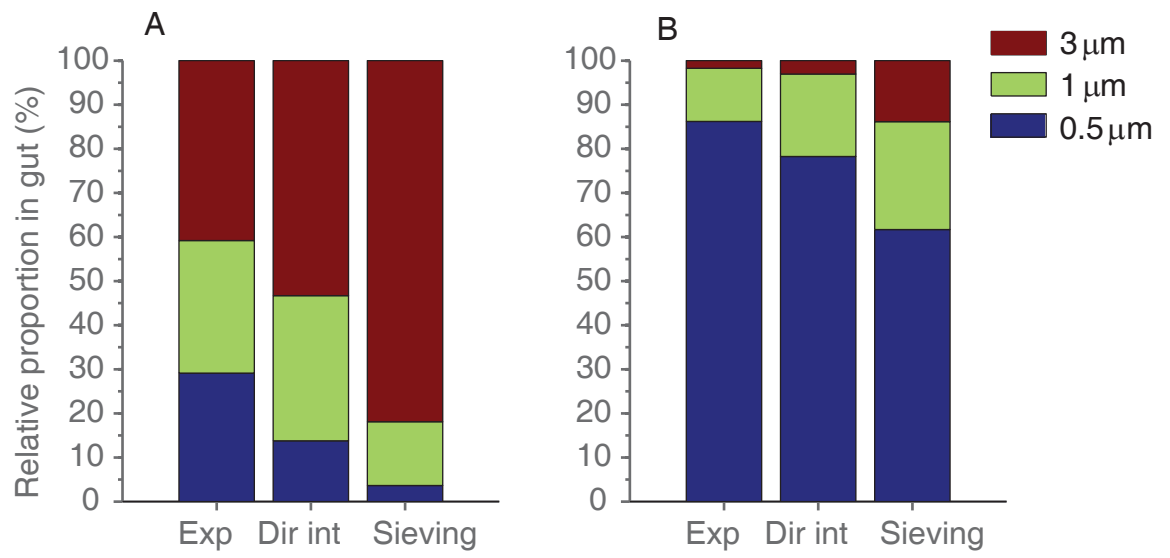
4











Individual	Stage	Body length, L_b (mm)	Mean speed, U (cm s^{-1})	Max speed (cm s^{-1})
1	Aggregate	27	2.3 ± 1.1 (3)	4.1
2	Solitary	30	1.2 ± 0.9 (9)	4.1
3	Solitary	34	1.5 ± 0.1 (15)	2.4
4	Solitary	53	1.9 ± 1.0 (13)	3.9
5	Solitary	56	2.0 ± 1.8 (11)	6.7
6	Solitary	62	0.8 ± 0.2 (14)	1.6
Mean \pm SD (n)			1.6 ± 0.6 (6)	3.8 ± 1.7 (6)

SUPPORTING INFORMATION

The efficiency of direct interception by a single fiber was computed as (12)

$$E_R = [2E_* \ln E_* - E_* + E_*^{-1}] / \Lambda, \quad [\text{S1}]$$

where

$$E_* = 1 + \frac{d_p}{d}, \quad [\text{S2}]$$

$$\Lambda = 1 - 2 \ln \tau + \frac{\tau^2}{6} - \frac{\tau^4}{144} + \frac{\tau^6}{1080}, \quad [\text{S3}]$$

$$\tau = \pi d \sqrt{W^2 + L^2} / (WL). \quad [\text{S4}]$$

W and L are width and length of the mesh opening, respectively, and d is the fiber diameter.

Direct interception efficiency reaches 100% when particle size is equal to mesh width. Although the model assumes $d_p \ll d$, the above expressions are still realistic as validated by several other studies where particles are larger than the mesh diameter (12, 17, 64).

The efficiency of diffusional deposition by a single fiber is (12):

$$E_D = 3.7 \Lambda^{-1/3} Pe^{-2/3} + 0.62 Pe^{-1}, \quad [\text{S5}]$$

where $Pe = dU/D$ is the Peclet number and D is the diffusion coefficient of the particles. For colloidal particles or non-motile organisms, diffusion arises from Brownian motion and $D = kT/(3\pi\rho\nu d_p)$, where $k = 1.38 \times 10^{-23} \text{ m}^2 \text{ kg s}^{-2} \text{ K}^{-1}$ is Boltzmann's constant and T is temperature. For motile microorganisms diffusivity results from random motility, increasing with swimming speed, and D was computed using the semi-empirical results of Visser and Kiørboe ($D = 2.8d_p^{1.71}$, D in $\text{cm}^2 \text{ s}^{-1}$ and d_p in cm , ref. 38).

Finally, the total efficiency of a rectangular filter, which was used in the calculations, is (12)

$$E = \frac{(E_R + E_D)d}{h_E} \left[1 - \frac{(E_R + E_D)d}{W + L} \right], \quad [\text{S6}]$$

where $h_E = WL/(W+L)$ is the equivalent mesh spacing.